

Article

Engineering the Biosynthesis of prFMN Promotes the Conversion between Styrene/CO₂ and Cinnamic Acid Catalyzed by the Ferulic Acid Decarboxylase Fdc1

Xiaoni Zhu, Hongfei Li, Jiangang Ren, Yanbin Feng  and Song Xue *

School of Bioengineering, Dalian University of Technology, Dalian 116024, China

* Correspondence: afyb@dlut.edu.cn (Y.F.); xuesong@dlut.edu.cn (S.X.)

Abstract: Enzymatic decarboxylation and carboxylation are emerging as prospective processes to produce high-value compounds under mild conditions. Ferulic acid decarboxylase Fdc1 catalyzes broad substrate tolerance against α , β -unsaturated carboxylic acids, and provides green routes for carbon dioxide fixation with the reversible carboxylation, while the activity of the enzyme is limited by the indispensable cofactor prenylated flavin (prFMN), which is unstable and is rarely detected in nature. In this study, a prFMN efficient synthesis route was built using six exogenous enzymes introduced into *E. coli* cells, leading to the construction of a powerful cell catalyst named SC-6. Based on the metabolic analysis, the results indicated that the reduction of FMN to FMNH₂ was the bottleneck in prFMN synthesis pathway, and introducing FMN reductase increased the production of prFMN 3.8-fold compared with the common flavin prenyltransferase UbiX overexpression strain. Using SC-6 cell catalyst, the decarboxylation activity of Fdc1 increased more than 20 times with cinnamic acid and 4-acetoxycinnamic acid as substrates. Furthermore, the reversible carboxylation reaction was carried out, and the cell catalyst presented 20 times carbon dioxide fixation activity using styrene to produce cinnamic acid. Finally, the maximum yield of cinnamic acid catalyzed by SC-6 achieved $833.68 \pm 34.51 \text{ mM}\cdot\text{mg}^{-1}$ in two hours. The constructed prFMN pathway in vivo provides fundamentals for efficient decarboxylation and carbon fixation reactions catalyzed by prFMN-dependent enzymes.

Keywords: cell catalyst; prFMN; decarboxylase; carboxylation; cinnamic acid



Citation: Zhu, X.; Li, H.; Ren, J.; Feng, Y.; Xue, S. Engineering the Biosynthesis of prFMN Promotes the Conversion between Styrene/CO₂ and Cinnamic Acid Catalyzed by the Ferulic Acid Decarboxylase Fdc1. *Catalysts* **2023**, *13*, 917. <https://doi.org/10.3390/catal13060917>

Academic Editors: Ruizhi Han and Gopal Patel

Received: 6 May 2023

Revised: 17 May 2023

Accepted: 22 May 2023

Published: 23 May 2023



Copyright: © 2023 by the authors. Licensee MDPI, Basel, Switzerland. This article is an open access article distributed under the terms and conditions of the Creative Commons Attribution (CC BY) license (<https://creativecommons.org/licenses/by/4.0/>).

1. Introduction

Enzymatic decarboxylation and carboxylation are essential reactions in both biological and chemical processes which take responsibility for carbon release and carbon fixation in nature [1,2]. Ferulic acid decarboxylase Fdc1 from *Aspergillus niger* and *Saccharomyces cerevisiae* has been characterized as catalyzing the decarboxylation of cinnamic acid derivatives with a broad substrate tolerance against α , β -unsaturated carboxylic acids, including aromatic, heteroaromatic, and unsaturated aliphatic acids [3,4]. Additionally, the reversible carboxylation of Fdc1 is attracting considerable attention as a green catalyst for carbon dioxide fixation and C–C bond-forming reactions under mild conditions [5].

Fdc1 belongs to the UbiD family, which is widely distributed in bacterial, archaeal, and fungal. UbiD is involved in the biosynthesis of ubiquinone in *E. coli* [6], while several UbiD family proteins have been shown to be active against heteroaromatic acids such as protocatechuic acid, 2,5-furandicarboxylic acid, 2-furoic acid, and phenylphosphate [7]. Particularly, these UbiD enzymes depend on the recently identified prenylated flavin mononucleotide (prFMN) cofactor for catalysis, with the conventional isoalloxazine of the flavin modified by the addition of a fourth ring derived from an isoprene unit. Thus, the unusual modification introduces a nitrogen ylide functionality into the ring system that converts this quintessential redox cofactor into one that supports (de)carboxylation reactions at sp²-hybridized carbon atoms [8]. In the case of Fdc1, reversible decarboxylation

has been suggested to occur via a 1,3-dipolar cycloaddition process between the substrate and the azomethine ylide portion of the prFMN cofactor [9].

Structural and biochemical studies have revealed the biosynthesis mechanisms of prFMN in *E. coli* cells. Firstly, the UbiX catalyzes the prenyltransfer from dimethylallyl(pyro)phosphate to reduced FMNH₂, yielding prFMNH₂, thus extending the FMNH₂ with the fourth nonaromatic ring. Subsequently, the UbiD binds the reduced prFMNH₂ from UbiX, and prFMNH₂ is suggested to undergo oxidative maturation to yield prFMN to the finally active form as prFMN^{iminium}. However, the preparations of prFMN are not commercially available, as the oxidative maturation process of prFMNH₂ by UbiD family enzymes (such as UbiD, Fdc1) to the active prFMN^{iminium} form appears prone to hydrolysis [10]. Moreover, oxygen exposure of the reduced prFMNH₂/UbiX complex results in the formation of derivative species such as prFMN C_{4a}-OOH, prFMN-OH, prFMN^{radical}, prFMN^{radical}-H, and so on [11]. These forms of prFMN have been proved to be inactive and unable to support the activity of the UbiD family proteins.

Due to the instability of prFMN, currently the supply of prFMN cofactor can be substituted by the use of multiple enzyme systems or crude cell lysates [12,13]. The supply and stability issue of the prFMN^{iminium} is still one of the major bottlenecks limiting the applicability of Fdc1. Recent studies have focused on the biosynthesis of the cofactor in vivo or in vitro [14]. However, in solution, the irreversible conversion and inactivation of prFMNH₂ hinders the activity of holo-Fdc1. More importantly, some existing forms of prFMN are difficult to determine by mass spectrometry, which increases the difficulty for directed synthesis of the active form of prFMN.

Though the intrinsic activity of Fdc1 is relatively low, recent studies have demonstrated that the conversion efficiency catalyzed by Fdc1 can be enhanced through aromatic C-H activation by constructing a non-natural route to corresponding acids and derivative compounds, and studies have also shown the potential of using Fdc1 in the production of 1,3-butadiene by molecular evolution of Fdc1 [15]. Based on protein engineering, the mutations around the active site including I189V provided improved activity of Fdc1 towards specific substrate analogues [16]. These prFMNs are utilized by the synthesis of endogenous UbiX and UbiD in *E. coli* cells, while the endogenous expression of UbiX and UbiD appears to be insufficient for activation of recombinant Fdc1, especially when Fdc1 is overexpressed, as confirmed by coexpression of UbiX and Fdc1 in vivo under aerobic conditions, enhanced the activity of Fdc1 from 0.6 U·mg⁻¹ to 1.5 U·mg⁻¹ [17]. Therefore, the lack of active forms of prFMN still needs to be improved to meet the prospective industrial applications.

Here, a highly efficient prFMN supply strain is constructed; based on the introduction of six exogenous enzymes into *E. coli* cells, a multiple enzyme cell system including ScFdc1 was generated and named SC-6. Mass spectrometry proved prFMN was enhanced by 3.8-fold compared to the commonly used UbiX and UbiD coexpression systems. Consequently, the catalytic activity of SC-6 strain increased 20 times using cinnamic acid as substrate in the decarboxylic process. Furthermore, the reversible carboxylation reaction using styrene and carbon dioxide to produce cinnamic acid was conducted, and the catalytic efficiency reached $833.68 \pm 34.51 \mu\text{M}\cdot\text{mg}^{-1}$ in two hours, which was the most efficient carbon fixation reported by Fdc1 at present.

2. Results

2.1. Reconstruction of the prFMN Biosynthesis Pathway in *E. coli*

The cofactor prFMN is catalyzed by UbiX using the reduced form of FMN and DMAP as substrates, and further undergoes oxidative maturation by UbiD family enzymes in *E. coli*. In addition, previously, it has been demonstrated that coexpression of UbiX promotes the activity of Fdc1. Then, we constructed PaUbiX and ScFdc1 onto the pETDuet vector and transformed them into *E. coli* cells, and the strain was named SC-2. Due to the insufficient supply of intracellular FMN and DMAP, the riboflavin kinase (RFK) domain of FAD synthetase, which catalyzes the riboflavin to FMN, and EcThiM, which catalyzes the prenyl

to DMAP, were introduced. With the supplementation of riboflavin and prenil during cell cultivation, the concentration of FMN and DMAP was supposed to be improved; thus, the SC-2 strain carrying pRSFDuet_EcThiM_CaRFK was named SC-4. However, the RFK domain of CaFADS converted the riboflavin to the oxidized form of FMN, to further convert FMN to the reductive form FMNH₂ as the direct substrate of UbiX, the flavin reductase Fre from *E. coli* was engineered into SC-4 as named SC-5. Taking consideration of the NADH recycling of Fre, the formate dehydrogenase FDH from *Pseudomonas* sp. 101 was further engineered into SC-5, and finally, the recombinant *E. coli* strain SC-6 was obtained. The construction of the enzymes and the strains is shown in Figure 1.

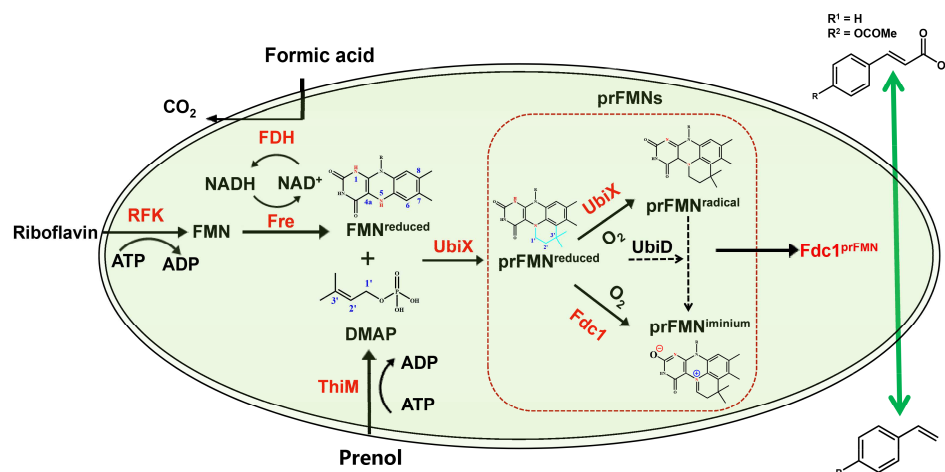


Figure 1. Schematic representation of the prFMN synthesis and NADH/NAD⁺ regeneration system in *E. coli*. RFK: Riboflavin Kinase domain of the flavin adenine dinucleotide synthetase from *Corynebacterium ammoniagenes* (UniProt No. Q59263 with residues 183–338); Fre: flavin mononucleotide reductase from *E. coli* (UniProt No. P0AEN1); UbiX: flavin prenyltransferase from *Pseudomonas aeruginosa* (UniProt No. Q9HX08); FDH: formate dehydrogenase from *Pseudomonas* sp. 101 (UniProt No. P33160); ThiM: prenil kinase from *E. coli* (UniProt No. P76423); and Fdc1: ferulic acid decarboxylase from *Saccharomyces cerevisiae* (UniProt No. Q03034). The green arrow represents the reversible reactions that were catalyzed by the cell catalyst in subsequent results. R¹ represents cinnamic acid and styrene, while R² represents 4-acetoxycinnamic acid and 4-acetoxystyrene.

2.2. The Engineered prFMN Strain Demonstrated High Decarboxylation Efficiency

ScFdc1 coexpressed with PaUbiX, with the former carrying the 6xHis-tag, was purified by Ni-NTA affinity chromatography and showed lower activity compared with the whole cell lysate. Then, the whole cell lysate was used as the catalyst in this study for the subsequent enzymatic activities. Firstly, the expression of the exogenous enzymes was confirmed by SDS-PAGE, as shown in Figure 2a. Using 5 mM cinnamic acid as decarboxylation substrate, the SC-2 lysate showed a conversion rate by 5% in 15 min, while the SC-4, including the EcThiM and CaRFK, presented a significant improvement with a conversion rate of 32%. Taking the SC-5 carrying the EcFre that converts FMN to FMNH₂ as the precursor of prFMNH₂, the decarboxylation rate reached 44%. Furthermore, the NADH regenerative cycle was introduced into SC-6, and the SC-6 demonstrated a final conversion rate of 62% in 15 min (Figure 2b). In consideration of the consumption of formic acid in the NADH regenerative cycle, 5 mM formic acid was additionally added in the step of cell lysis process, while no significant improvement was observed. It should be noted that the expression proportion of ScFdc1 is about 13.4% of the total protein in SC-2 calculated by grayscale integral; while, due to the presence of multiple expression vectors in SC-6, ScFdc1 accounts for 5.7% of total proteins. For calculation here, we use the same volume of cell lysate, so the actual usage of ScFdc1 in SC-6 is relatively lower than that in SC-2, which further indicates that the ScFdc1 expressed in SC-6 would present much higher activities.

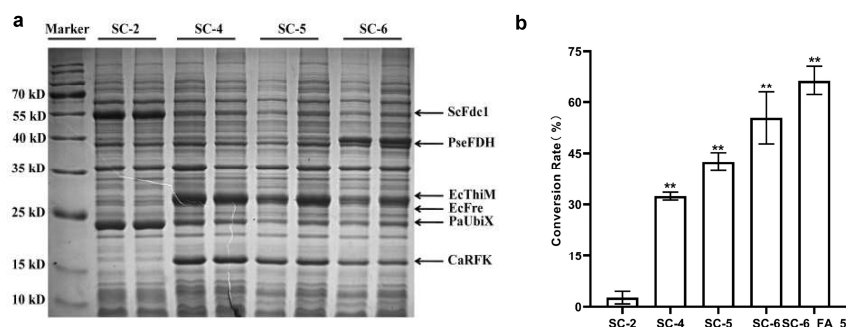


Figure 2. Decarboxylation of cinnamic acid using *E. coli* cell catalyst. (a) Protein expression and SDS-PAGE of the exogenous enzymes in *E. coli* cell lysis. The ScFdc1, PseFDH, EcThiM, EcFre, PaUbiX, and CaRFK were calculated with theoretical molecular weights of 56.2 kD, 44.2 kD, 27.3 kD, 26.3 kD, 22.4 kD, and 17.2 kD, respectively. The molecular weights of EcThiM and EcFre are similar, and the expression level of EcFre is lower than that of EcThiM, so the band of EcFre is not clear while has been further conformed. The content of Fdc1 in whole cell lysate was calculated by grayscale integrals, with two sets of experiments repeated. (b) Decarboxylation of cinnamic acid with different recombinant *E. coli* strains in 15 min. The vertical axis represents the substrate conversion rate of cinnamic acid. Values are presented as mean \pm SD ($n = 3$). Significant results were compared with SC-2, with significance difference indicated (“***”: $p < 0.01$).

2.3. Kinetic Parameters of SC-2 and SC-6 Cell Catalysts with Cinnamic Acid and 4-Acetoxy-cinnamic Acid as Substrates

To further analyze the improvement of decarboxylation activity between SC-2 and SC-6, the steady-state kinetic parameters of the two engineered strains were determined by measuring their initial velocity. The V_{\max} of SC-2 and SC-6 for the decarboxylation of cinnamic acid were 0.23 ± 0.03 and $11.79 \pm 0.67 \mu\text{mol}\cdot\text{s}^{-1}\cdot\text{mg}^{-1}$, respectively, with a 51-fold increment, as shown in Figure 3a. The K_m was $197.63 \pm 33.81 \mu\text{M}$ for SC-6 and $81.17 \pm 5.93 \mu\text{M}$ in contrast with SC-2, indicating that engineering the biosynthesis of prFMN significantly improved the catalytic efficiency of ScFdc1, while presenting a certain impact of ScFdc1 on the substrate binding affinity with cinnamic acid.

Fdc1 has been identified with broad substrate selectivity. 4-acetoxystyrene, the decarboxylation product of 4-acetoxy-cinnamic acid, is mainly used in the synthesis of polyhydroxystyrene as the main component of photoresist resin. Using 4-acetoxy-cinnamic acid as substrate, the SC-6 demonstrated excellent activity compared with SC-2, as shown in Figure 3b. The V_{\max} of SC-2 and SC-6 for the decarboxylation of 4-acetoxystyrene were 0.11 ± 0.002 and $3.20 \pm 0.11 \mu\text{mol}\cdot\text{s}^{-1}\cdot\text{mg}^{-1}$, with a 29.1-fold increment. In addition, the K_m was 219.77 ± 11.93 for SC-6 and $269.35 \pm 19.16 \mu\text{M}$ for SC-2. In brief, the results clearly demonstrated that introducing the prFMN synthesis pathway and NADH regeneration cycle promoted the catalytic efficiency of ScFdc1.

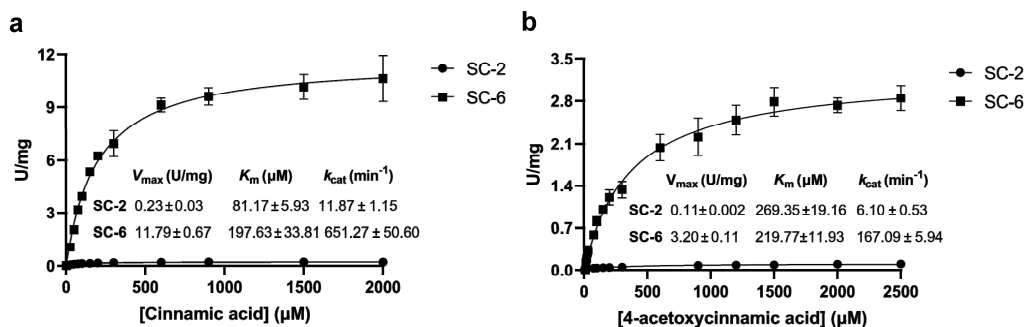


Figure 3. (a) Kinetic parameters using SC-2 and SC-6 as cell catalyst with cinnamic acid as substrate. (b) Kinetic parameters using SC-2 and SC-6 as cell catalyst with 4-acetoxy-cinnamic acid as substrate. Data are presented as mean \pm SD ($n = 3$).

2.4. Semi-Quantitative Analysis of FMN and prFMN by Native Mass Spectrometry

To quantify the biosynthesis process of prFMN, the cofactor quantitative analysis of the recombinant strain was performed on a liquid chromatograph mass spectrometer. The reductive forms of FMNH₂ and prFMNH₂ are reported to be unstable for analysis, while the oxidation forms of FMN and prFMN can be relatively determined. Due to the fact that FMN can be produced in wild type *E. coli* cells, the FMN content in *E. coli* (DE3) cells was set for background control at 100%; similarly, the response value of prFMN in *E. coli* (DE3) cells was defined at 100% due to the endogenous EcUbiX and EcUbiD in *E. coli* being able to produce prFMN.

In comparison to the *E. coli* wild type strain, the FMN content in SC-2 carrying PaUbiX and ScFdc1 was elevated by 52 times (Figure 4a), indicating the accumulation of oxidized form of FMN, while the prFMN was only elevated to 110% compared to wild type cell strain (Figure 4b). Furthermore, CaRFK was introduced which directly catalyzed riboflavin to FMN, and EcThiM catalyzed the conversion of prenyl to DMAP. The SC-4 strain improved FMN accumulation by 384 times and prFMN accumulation by 1.3 times, indicating the reduction of FMN to the reductive form would be the rate-limiting step. Thus, the FMN reductase was introduced in SC-5 and the FMN accumulation showed a minor increase compared with SC-4, while the prFMN abundance improved 2-fold compared to SC-4. Further engineering of FDH improved prFMN by 3.5 times and promoted the FMN pathway with FMN accumulation by 851 times. To improve FMN reductase by NADH regeneration, formic acid was additionally brought into the system, and the FMN concentration in SC-6 plus formic acid declined compared to SC-6, while a slight improvement was obtained by SC-6 plus formic acid, with the production of prFMN increasing by 10% compared to SC-5 strain.

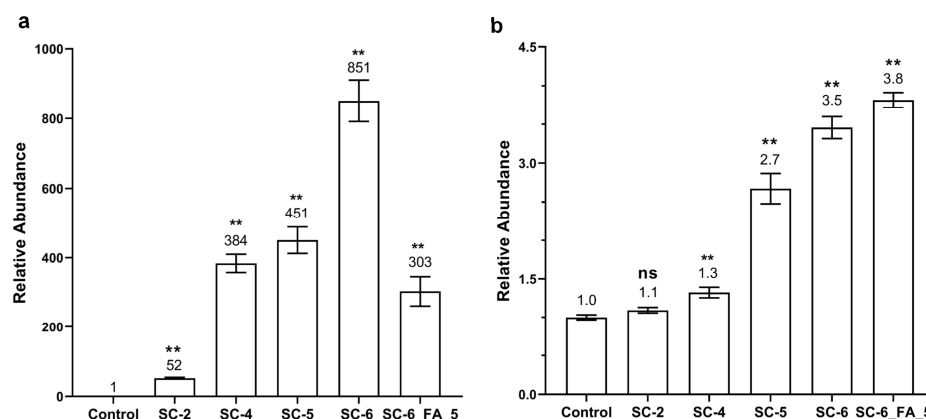


Figure 4. Mass spectrometry analysis of FMN metabolism in recombinant *E. coli* strains. (a) Relative abundance of FMN. (b) Relative abundance of prFMN. Control refers to the endogenous background in the *E. coli* BL21 (DE3) strain, and SC-6-5 mM refers to SC-6 with a supplement of 5 mM formate during cell culture. Values are presented as mean \pm SD ($n = 3$). Significant results were compared with control, with significance difference indicated (“ns”: no significance; “**”: $p < 0.01$).

2.5. Biosynthesis of the prFMN Promotes Carbon Fixation on Styrene Catalyzed by ScFdc1

Fdc1 was reported to be capable of catalyzing the synthesis of cinnamic acid by styrene carboxylation, while the product merely stayed at the detectable level without reporting a specific yield [18]. Using SC-2 as the catalyst, the styrene was converted to cinnamic acid by a rate of $0.86 \pm 0.17 \text{ Mm}\cdot\text{h}^{-1}\cdot\text{mg}^{-1}$ at 0.5 M KHCO₃ overnight. While using SC-6 as the catalyst, it achieved a productivity of cinnamic acid of $42.17 \pm 1.80 \mu\text{M}\cdot\text{h}^{-1}\cdot\text{mg}^{-1}$ (Figure 5a). Moreover, the concentration of KHCO₃ as the carboxylation buffer was optimized to achieve a productivity of cinnamic acid by $74.61 \pm 2.15 \mu\text{M}\cdot\text{h}^{-1}\cdot\text{mg}^{-1}$ under 2.7 M KHCO₃. Different from the reported conditions of pressured carbon dioxide and overnight reactions, the reaction time was optimized, and it was found that the yield reached the maximum in two hours instead of overnight (Figure 5b). The results indicated

that extending the time for carboxylation is unnecessary and may be time-consuming, which would be hindered by the potential decarboxylation process. Finally, increasing the amount of the cell catalyst by five times achieved a maximum yield of cinnamic acid of $833.68 \pm 34.51 \mu\text{M}\cdot\text{mg}^{-1}$ in 2 h.

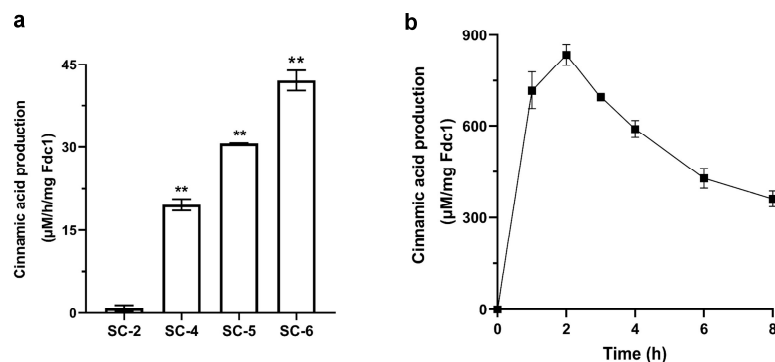


Figure 5. (a) Carboxylation of styrene for different recombinant cell catalyst containing ScFdc1 overnight. Values are presented as mean \pm SD ($n = 3$). Significant results were compared with SC-2, with significance difference indicated (“***”: $p < 0.01$). (b) A time profile of carboxylation of styrene catalyzed by SC-6 containing ScFdc1. Data are presented as mean \pm SD ($n = 3$).

3. Discussion

Enzymatic carboxylation is emerging as an attractive and green route to produce high value carboxylic acids under mild conditions. In particular, divalent metal ion-independent decarboxylases, represented by 2,3-dihydroxybenzoic acid decarboxylase [19] and salicylic acid decarboxylase [20], catalyze the conversion of substrates such as catechol to hydroxybenzoic acid, and the substrate conversion rate could reach 60% under conditions such as CO_2 pressure [21]. In addition, by removing products or adding quaternary ammonium salts, the reaction equilibrium is moved towards the CO_2 fixing direction, and the substrate conversion rate can reach up to 90% or even higher [22]. However, the above enzymes are limited to phenolic substrates and require the assistance of ortho hydroxyl groups for selective carboxylation.

Ferulic acid decarboxylase catalyzes the decarboxylation of ferulic acid to form 4-ethylene guaiacol in the biological metabolic pathway. It was found that the enzyme is capable of catalyzing the decarboxylation and reversible carboxylation processes of (aromatic) acrylic acid derivatives, such as the carboxylation of nearly forty substrates such as epoxy derivatives, aromatic olefins, and aliphatic olefins [23]. Moreover, the prFMN cofactor of Fdc1 does not involve redox state change or cofactor regeneration in the reaction process, which conforms to the characteristics of green biological manufacturing. Therefore, prFMN-dependent Fdc1 and its homologous enzymes have become hot spots in the utilization of CO_2 resources and biotransformation.

However, due to the thermodynamic barrier associated, as well as the high energy requirement for substrate activation, enzymatic CO_2 fixation routes are rarely efficient [24]. For example, with styrene and carbon dioxide as substrates, under buffer conditions such as 0.1–2.7 M KHCO_3 or $(\text{NH}_4)_2\text{HCO}_3$, and whole cells expressing Fdc1 enzymes as catalysts, the substrate conversion efficiency is limited at the detection line level only after 18 h of reaction at 30°C . In addition, enhanced biocatalyst loading ($100 \text{ mg whole cells mL}^{-1}$) and CO_2 (30 bar) produced small amounts of carboxylation products [25]. Similarly, enzymatic characterization of the prFMN-containing decarboxylase TtnD presented the k_{cat} in less than 1 min^{-1} [26]. Additionally, the enzyme catalyzed para-carboxylation of catechols by AroY that belongs to the UbiD enzyme family showed low activity [27].

Dozens of UbiD family enzymes are being excavated, pointing out the stability and indispensability of prFMN cofactor [28]. The pyrrole-2-carboxylic acid decarboxylase PA0254 expressed in the absence of UbiX possessed little or no activity, while supplying the cofactor reactivated the enzyme [29]. Cofactor engineering has been emphasized as an important

strategy for the microbial production of natural products. Engineering FAD and NADPH cofactor strategies have been developed for rewiring biosynthesis, compartmentalization, and recycling, which enable the highest production of ferulic acid in microbial cell factories [30]. In addition, metabolic engineering of the FAD biosynthesis pathway in *E. coli* also provides an effective strategy for improving whole cell catalytic capability for one-step production of α -keto acids from L-amino acids [31].

Since the host *E. coli* cells contain the endogenous UbiX, the whole cells of *E. coli* BL21 (DE3) pLysS only overexpressing ScFdc1 have been used as the catalyst to perform the decarboxylation of ferulic acid with a conversion rate of about 10% in an hour at 2 mM substrate concentration [32]. We constructed the SC-2, including the PaUbiX and ScFdc1, and the cell lysate showed a conversion rate of 5% in 15 min with 5 mM cinnamic acid. To improve the content of the cofactor, the SC-6 strain, including FMN precursor supply, FMN reduction, and NADH regeneration modules, was reconstructed, and the engineered strain showed a final conversion rate of 62% within 15 min, and the substrates could be completely transformed by extending the reaction time. The experiment was conducted using the same volume of the cell lysate, considering the ScFdc1 expression level in SC-6 is about 2.3 times lower than in SC-2, the enzymatic activities of ScFdc1 in SC-6 should be much higher. The results indicated that increasing the content of the prFMN cofactor could significantly enhance the activity of Fdc1. Based on the engineered prFMN pathway in SC-6, it was demonstrated that the catalytic activity of substrates including cinnamic acid and 4-acetoxycinnamic acid was remarkably elevated, i.e., by more than 22- and 38-fold, calculated by k_{cat}/K_m . These results suggest that a highly efficient prFMN supply strain has the potential to improve the catalytic activities for the prFMN-dependent decarboxylases and carboxylases.

Currently, the intermediate metabolite quantification in the biosynthesis process of prFMN has been rarely studied. Previous studies established a linear one-pot enzyme cascade for in vitro generation of prFMN; the results demonstrated that the prenyl phosphorylation to DMAP step by ThiM appears to represent the major bottleneck limiting the rate of FMN prenylation and UbiD activation [17]. Similarly, FMN prenylation was reported to be limited by intracellular levels of DMAP and FMN in *E. coli* cells, which can be improved by adding prenyl and riboflavin to the cell cultures [33]. However, our in vivo results, determined by mass spectrometry in this study, showed that the SC-4 strain improved the FMN accumulation by 384 times, while prFMN accumulation only increased by 1.3 times. It was considered that the reduction of FMN to the reductive form, FMNH₂, would be the rate-limiting step, as the reduced FMNH₂ was the direct substrate of UbiX, producing the reduced form of prFMNH₂. Actually, to solve the low conversion rate of FMN to the reductive form FMNH₂, the FMN reductase was introduced in SC-5 and improved the productivity of prFMNH₂ by two times compared with SC-4. Even though the content of prFMNH₂ was promoted, it was indicated that the catalytic efficiency of FMN reductase is still insufficient compared with the increment of FMN by 451 times.

Fdc1 has been used as a reversible enzyme to fix carbon dioxide for valuable compounds. To improve the carboxylation efficiency of the reversible decarboxylases, efforts have been made to resolve the limitations. An excess of bicarbonate is usually required as the CO₂ source, or the fixed carbon substrate CO₂ is pressurized as the reaction condition. In addition, the addition of quaternary ammonium salts to induce the precipitation of corresponding carboxylation products can also improve the conversion efficiency of substrates via the in situ removal of products through the ion exchange method. Recently, researchers have coupled multiple enzyme systems, such as through coupling with carboxylate reductase, to achieve the production of downstream aldehydes, amines, amides, and alcohols. This process uses ATP as the energy donor and NADH as the reducing force, and ultimately converts styrene into cinnamyl alcohol to improve the conversion rate of styrene substrates [18]. Taking consideration of the carboxylation process in this study, the SC-6 demonstrated efficient activity enhancement by about 10-times with the conversion rate up to 0.63% with 10 mM styrene. Although the carboxylation reaction of ScFdc1 also

shows a corresponding enhancement in activity, the productivity of cinnamic acid is still far from industrial applications. Combining cofactor engineering, directed evolution of the enzyme and process optimization may ultimately result in carbon fixation for high-value compounds to meet industrial demands.

4. Materials and Methods

4.1. Strains, Plasmids, and Chemicals

The *E. coli* strain BL21 (DE3) was used as the host for the production of enzymes associated with the synthesis of prFMN. Molecular biology enzymes (LA Taq DNA polymerase, BamH I, Hind III, Nde I and Xho I) were purchased from Takara Biomedical Technology Co. (Beijing, China), and common kits (gel extraction, plasmid isolation, DNA ligation and competent cell preparation) were provided by Sangon Co., Ltd. (Shanghai, China). All chemical reagents were purchased from Sangon Co., Ltd. (Shanghai, China), with the exception of cinnamic acid, styrene, prenol and riboflavin, which were provided by Aladdin Biochemical Technology Co., Ltd. (Shanghai, China).

4.2. Engineering of the prFMN Biosynthesis Pathway in *E. coli* Cells

The genes encoding *fdc* and *ubix* from *S. cerevisiae* and *P. aeruginosa* were synthesized and cloned into the expression vector pACYCDuet. The *E. coli* prenol kinase gene (*thim*) and the *C. ammoniagenes* riboflavin kinase gene (*rflk*) were synthesized and cloned into the pRSFDuet vector. The FMN reductase *Fre* from *E. coli* and the formate dehydrogenase *FDH* from *Pseudomonas* sp. 101 were PCR amplified from genomic DNA. In addition, the PCR products were digested with restriction enzymes and ligated onto the pETDuet vector. The resulting constructs were transformed into *E. coli* strain BL21 (DE3) for protein expression. The recombinant strain carrying PaUbiX and ScFdc1 was named SC-2. The SC-4, SC-5, and SC-6 of the recombinant *E. coli* strains used in the present study were named and listed in Table 1.

Table 1. Strains and plasmids used in the study.

Strains	Experimental Group
SC-2	<i>E. coli</i> BL21 (DE3) containing the recombinant plasmid pACYCDuet_PaUbiX_ScFdc1
SC-4	SC-2 containing the recombinant plasmid pRSFDuet_EcThiM_CaRfK
SC-5	SC-4 containing the recombinant plasmid pETDuet_EcFre
SC-6	SC-4 containing the recombinant plasmid pETDuet_EcFre_PsFDH
SC-6_FA_5	SC-6 with supplementing 5 mM formate during cell culture

4.3. Preparation of the Biocatalyst

The engineered *E. coli* strain was inoculated into 10 mL of Luria–Bertani medium supplemented with the appropriate antibiotics and cultivated on a rotary shaker with 220 rpm at 37 °C overnight. Ampicillin, kanamycin, or chloramphenicol with 50 µg·mL⁻¹ working concentration were added to the medium for selection depending on the vectors harbored by *E. coli*. After that, 1% (*v/v*) seed culture was inoculated into 1 L of Luria–Bertani medium containing the appropriate antibiotics, and *E. coli* cultures were grown at 37 °C and 220 rpm in a rotary shaker. When the optical density OD₆₀₀ of the culture reached 0.6–0.8, the strains were induced by isopropyl β-D-thiogalactoside (IPTG) to a final concentration of 0.2 mM. Furthermore, SC-4, SC-5, and SC-6 were supplemented with prenol at 1 mM and riboflavin at 0.1 mM final concentration. SC-6 also needed to add formate to a final concentration of 5 mM on this basis. Following overnight incubation at 16 °C and 220 rpm, cells were harvested via centrifugation at 5000 × *g* for 15 min at 4 °C. Then, the cell pellet was obtained from 50 mL of 1 L *E. coli* liquid maintained at −20 °C for further study. The cells were then resuspended in 5 mL Lysis buffer (50 mM phosphate buffer, pH 6.0 for decarboxylation or pH 7.5 for carboxylation) and broken using an ultrasonic cell disruptor. Biomass concentration was checked with the Bradford method, and SDS-PAGE using gray-level integration.

4.4. Pretreatment of the Cell Lysate for Mass Spectrometry Assay

The 50 mL of cultivated *E. coli* cells were harvested by centrifugation at 5400 rpm at 4 °C for 10 min. Then, 3 mL buffer including 50 mM NaPi (pH 6.0) and 50 mM sodium chloride were added for re-suspending the cell pellets. The ultrasonic disruption of the cell was performed at 300 W for 2 min by circulation of 2 s-work and 4 s-break. After that, 400 µL of the broken cell suspensions was drawn into a brown tube containing 1.2 mL methanol for protein precipitation and centrifugation. Finally, the supernatant was drawn into a brown injection bottle after centrifugation at 12,000 rpm at 4 °C for 10 min and stored at −20 °C.

4.5. Intracellular Analysis of the Possible Forms of prFMNs Using LC-MS

For LC-MS analysis, an ultra-high performance liquid chromatograph (Waters, MA, USA) was used coupled to a tripleTOF™ 5600 plus (Applied Biosystems, Waltham, CA, USA) mass spectrometer equipped with an electrospray source. An aliquot of 10 µL supernatant was injected into a BEH C8 (100 mm × 2.1 mm × 1.7 µm, Waters, MA, USA) column. The column temperature was set at 30 °C, with a flow rate of 0.25 mL·min^{−1}. The gradient started with 40% B (methanol), maintained for 8 min, then linearly increased to 95% B within 4.5 min, and was maintained at 95% B until 16 min. Then, the elute phase proportion was rapidly set back to 60% A (0.01% ammonia and 10 mM ammonium acetate in water) within 0.5 min, and the total run time for each analysis was 20 min, including a post-equilibration of 3.5 min. For data acquisition, the m/z scanning was from 400 to 800 Dalton in ESI negative ionization mode. The ion source parameters were set as follows: the source temperature was set at 500 °C; gas 1 and gas 2 at 0.28 MPa; the curtain gas at 0.24 MPa; and the floating ion spray voltage was −4.5 kV.

4.6. Enzymatic Decarboxylation Catalyzed by the ScFdc1 Whole Cell Lysate

The decarboxylation activity assays were performed in 1.5 mL brown eppendorf tubes to avoid light with a reaction volume of 200 µL, which was undertaken in 50 mM sodium phosphate buffer, pH 6.0. Stock solutions of substrate cinnamic acid were dissolved in acetonitrile. The reaction system contained 5 mM cinnamic acid and 40 µL cell lysate (50 mL cells resuspended in 5 mL Lysis buffer, about 5–10 µg ScFdc1 in the whole-cell catalyst calculated using grayscale integral), and the mixture was incubated at 30 °C. The reaction was suspended by adding 600 µL acetonitrile and centrifuged at 12,000 × g for 5 min to remove insoluble material. Samples were quantified on a high-performance liquid chromatography system (Infinity II, Agilent 1260, Santa Clara, CA, USA) equipped with an ultraviolet detector at 254 nm and an Eclipse XDB-C18 (250 × 4.6 mm, Agilent, Santa Clara, CA, USA) at a column temperature of 25 °C. The mobile phase was 50% (v/v) acetonitrile and 0.1% (v/v) trifluoroacetate in deionized water, and the injection volume of each sample was 5 µL, with a flow rate of 1.0 mL·min^{−1}.

4.7. Kinetic Parameters of ScFdc1 with Cinnamic Acid and 4-Acetoxy-cinnamic Acid

The kinetics parameters of enzymes were conducted in 200 µL standard reaction mixture consisting of 50 mM sodium phosphate buffer, pH 6.0, 0–2.5 mM cinnamic acid, and about 1 µg ScFdc1 in the whole cell catalyst for SC-6 and 10 µg ScFdc1 for SC-2. The conversion of substrate to product was determined using a standard curve of cinnamic acid. Steady-state kinetic parameters were determined at 30 °C for 5 min with various substrate concentrations using initial rate data from the Michaelis–Menten equation. For 4-acetoxy-cinnamic acid, 3 µg ScFdc1 in the whole cell catalyst for SC-6, and 15 µg ScFdc1 for SC-2 whole cell catalyst were used, respectively.

4.8. Enzymatic Carboxylation of Styrene

The conversion of styrene to cinnamic acid was carried out in a 200 µL reaction mixture containing 10 mM styrene, about 50 µg ScFdc1 in the whole cell catalyst, and 0.5 M KHCO₃, pH 8.3. Reaction mixtures in 1.5 mL eppendorf tubes were incubated at 30 °C for 2, 4,

6, 8 h, and overnight, after which the enzyme was inactivated by three times volume of acetonitrile. Samples were centrifuged before loading onto the HPLC system.

4.9. Statistical Analysis

All the measurements of the values used in this study represented the average \pm SD of individual replicates during the whole experiment. The unpaired T-tests analysis was performed in GraphPad Prism 8.0.2 software to conduct a significance analysis for (de)carboxylase activity determination and the possible forms of prFMNs content of different recombinant cell catalyst containing ScFdc1. A p value of less than 0.05 ($p < 0.05$) was considered statistically significant.

5. Conclusions

In this study, a highly efficient prFMN synthesis pathway *in vivo* was constructed. Metabolite analysis of the engineered *E. coli* cells SC-6 proved that the reduction of FMN to FMNH₂ is the bottleneck in prFMN biosynthesis pathway, and overexpression of the exogenous enzymes including Fre in *E. coli* led to a final enhancement of prFMN by 3.8-fold compared to the traditional UbiX-UbiD systems. Consequently, the engineered cells were used as the cell catalyst, and the SC-6 including ScFdc1 increased decarboxylation and carboxylation activities more than 20-fold. The results highlight a new approach to engineering the prFMN pathway in *E. coli*, i.e., a prospective path to prFMN-dependent enzymes.

Author Contributions: Conceptualization, X.Z., Y.F. and S.X.; methodology X.Z., H.L. and J.R.; writing—review and editing, X.Z., Y.F. and S.X. All authors have read and agreed to the published version of the manuscript.

Funding: This research was funded by the National Key Research and Development Program, grant number: 2021YFC2103702; and Fundamental Research Funds for the Central Universities, grant number: DUT22LK03.

Data Availability Statement: Data of this study are available in the article.

Conflicts of Interest: The authors declare no conflict of interest.

References

1. Bierbaumer, S.; Nattermann, M.; Schulz, L.; Zschoche, R.; Erb, T.J.; Winkler, C.K.; Tinzl, M.; Glueck, S.M. Enzymatic Conversion of CO₂: From Natural to Artificial Utilization. *Chem. Rev.* **2023**, *123*, 5702–5754. [[CrossRef](#)] [[PubMed](#)]
2. Plasch, K.; Resch, V.; Hitce, J.; Poplonski, J.; Faber, K.; Glueck, S.M. Regioselective Enzymatic Carboxylation of Bioactive (Poly)phenols. *Adv. Synth. Catal.* **2017**, *359*, 959–965. [[CrossRef](#)] [[PubMed](#)]
3. Payer, S.E.; Faber, K.; Glueck, S.M. Non-Oxidative Enzymatic (De)Carboxylation of (Hetero)Aromatics and Acrylic Acid Derivatives. *Adv. Synth. Catal.* **2019**, *361*, 2402–2420. [[CrossRef](#)] [[PubMed](#)]
4. Bhuiya, M.W.; Lee, S.G.; Jez, J.M.; Yu, O. Structure and Mechanism of Ferulic Acid Decarboxylase (FDC1) from *Saccharomyces cerevisiae*. *Appl. Environ. Microbiol.* **2015**, *81*, 4216–4223. [[CrossRef](#)]
5. Payne, K.A.P.; Marshall, S.A.; Fisher, K.; Cliff, M.J.; Cannas, D.M.; Yan, C.Y.; Heyes, D.J.; Parker, D.A.; Larrosa, I.; Leys, D. Enzymatic Carboxylation of 2-Furoic Acid Yields 2,5-Furandicarboxylic Acid (FDCA). *ACS Catal.* **2019**, *9*, 2854–2865. [[CrossRef](#)] [[PubMed](#)]
6. Marshall, S.A.; Fisher, K.; Cheallaigh, A.N.; White, M.D.; Payne, K.A.P.; Parker, D.A.; Rigby, S.E.J.; Leys, D. Oxidative Maturation and Structural Characterization of Prenylated FMN Binding by UbiD, a Decarboxylase Involved in Bacterial Ubiquinone Biosynthesis. *J. Biol. Chem.* **2017**, *292*, 4623–4637. [[CrossRef](#)]
7. Datar, P.M.; Marsh, E.N.G. Decarboxylation of Aromatic Carboxylic Acids by the Prenylated-FMN-dependent Enzyme Phenazine-1-carboxylic Acid Decarboxylase. *ACS Catal.* **2021**, *11*, 11723–11732. [[CrossRef](#)]
8. Marshall, S.A.; Payne, K.A.P.; Fisher, K.; White, M.D.; Cheallaigh, A.N.; Balaikaite, A.; Rigby, S.E.J.; Leys, D. The UbiX flavin prenyltransferase reaction mechanism resembles class I terpene cyclase chemistry. *Nat. Commun.* **2019**, *10*, 2357. [[CrossRef](#)]
9. Bailey, S.S.; Payne, K.A.P.; Saaret, A.; Marshall, S.A.; Gostimskaya, I.; Kosov, I.; Fisher, K.; Hay, S.; Leys, D. Enzymatic control of cycloadduct conformation ensures reversible 1,3-dipolar cycloaddition in a prFMN-dependent decarboxylase. *Nat. Chem.* **2019**, *11*, 1049–1057. [[CrossRef](#)]
10. Balaikaite, A.; Chisanga, M.; Fisher, K.; Heyes, D.J.; Spiess, R.; Leys, D. Ferulic Acid Decarboxylase Controls Oxidative Maturation of the Prenylated Flavin Mononucleotide Cofactor. *ACS Chem. Biol.* **2020**, *15*, 2466–2475. [[CrossRef](#)]

11. Wang, P.H.; Khusnutdinova, A.N.; Luo, F.; Xiao, J.; Nemr, K.; Flick, R.; Brown, G.; Mahadevan, R.; Edwards, E.A.; Yakunin, A.F. Biosynthesis and Activity of Prenylated FMN Cofactors. *Cell Chem. Biol.* **2018**, *25*, 560–570. [[CrossRef](#)] [[PubMed](#)]
12. Gahloth, D.; Fisher, K.; Payne, K.A.P.; Cliff, M.; Levy, C.; Leys, D. Structural and biochemical characterization of the prenylated flavin mononucleotide-dependent indole-3-carboxylic acid decarboxylase. *J. Biol. Chem.* **2022**, *298*, 101771. [[CrossRef](#)]
13. Saaret, A.; Villiers, B.; Stricher, F.; Anissimova, M.; Cadillon, M.; Spiess, R.; Hay, S.; Leys, D. Directed evolution of prenylated FMN-dependent Fdc supports efficient *in vivo* isobutene production. *Nat. Commun.* **2021**, *12*, 5300. [[CrossRef](#)] [[PubMed](#)]
14. Marshall, S.A.; Fisher, K.; Leys, D. The In Vitro Production of prFMN for Reconstitution of UbiD Enzymes. *Methods Mol. Biol.* **2021**, *2280*, 219–227. [[PubMed](#)]
15. Mori, Y.; Noda, S.; Shirai, T.; Kondo, A. Direct 1,3-butadiene biosynthesis in *Escherichia coli* via a tailored ferulic acid decarboxylase mutant. *Nat. Commun.* **2021**, *12*, 2195. [[CrossRef](#)] [[PubMed](#)]
16. Duta, H.; Filip, A.; Nagy, L.C.; Nagy, E.Z.A.; Totos, R.; Bencze, L.C. Toolbox for the structure-guided evolution of ferulic acid decarboxylase (FDC). *Sci. Rep.* **2022**, *12*, 3347. [[CrossRef](#)]
17. Batyrova, K.A.; Khusnutdinova, A.N.; Wang, P.H.; Di Leo, R.; Flick, R.; Edwards, E.A.; Savchenko, A.; Yakunin, A.F. Biocatalytic In Vitro and In Vivo FMN Prenylation and (De)carboxylase Activation. *ACS Chem. Biol.* **2020**, *15*, 1874–1882. [[CrossRef](#)]
18. Aleku, G.A.; Saaret, A.; Bradshaw-Allen, R.T.; Derrington, S.R.; Titchiner, G.R.; Gostimskaya, I.; Gahloth, D.; Parker, D.A.; Hay, S.; Leys, D. Enzymatic C-H activation of aromatic compounds through CO₂ fixation. *Nat. Chem. Biol.* **2020**, *16*, 1255–1260. [[CrossRef](#)]
19. Song, M.K.; Zhang, X.M.; Liu, W.D.; Feng, J.H.; Cui, Y.F.; Yao, P.Y.; Wang, M.; Guo, R.T.; Wu, Q.Q.; Zhu, D.M. 2,3-Dihydroxybenzoic Acid Decarboxylase from *Fusarium oxysporum*: Crystal Structures and Substrate Recognition Mechanism. *Chembiochem* **2020**, *21*, 2950–2956. [[CrossRef](#)]
20. Sheng, X.; Patskovsky, Y.; Vladimirova, A.; Bonanno, J.B.; Almo, S.C.; Himo, F.; Raushel, F.M. Mechanism and Structure of gamma-Resorcyolate Decarboxylase. *Biochemistry* **2018**, *57*, 3167–3175. [[CrossRef](#)]
21. Plasch, K.; Hofer, G.; Keller, W.; Hay, S.; Heyes, D.J.; Dennig, A.; Glueck, S.M.; Faber, K. Pressurized CO₂ as a carboxylating agent for the biocatalytic ortho-carboxylation of resorcinol. *Green Chem.* **2018**, *20*, 1754–1759. [[CrossRef](#)] [[PubMed](#)]
22. Ren, J.; Yao, P.Y.; Yu, S.S.; Dong, W.Y.; Chen, Q.J.; Feng, J.H.; Wu, Q.Q.; Zhu, D.M. An Unprecedented Effective Enzymatic Carboxylation of Phenols. *ACS Catal.* **2016**, *6*, 564–567. [[CrossRef](#)]
23. Lai, Y.; Chen, H.; Liu, L.; Fu, B.; Wu, P.; Li, W.; Hu, J.; Yuan, J. Engineering a Synthetic Pathway for Tyrosol Synthesis in *Escherichia coli*. *ACS Synth. Biol.* **2022**, *11*, 441–447. [[CrossRef](#)] [[PubMed](#)]
24. Aleku, G.A.; Roberts, G.W.; Titchiner, G.R.; Leys, D. Synthetic Enzyme-Catalyzed CO₂ Fixation Reactions. *Chemsuschem* **2021**, *14*, 1781–1804. [[CrossRef](#)]
25. Aleku, G.A.; Prause, C.; Bradshaw-Allen, R.T.; Plasch, K.; Glueck, S.M.; Bailey, S.S.; Payne, K.A.P.; Parker, D.A.; Faber, K.; Leys, D. Terminal Alkenes from Acrylic Acid Derivatives via Non-Oxidative Enzymatic Decarboxylation by Ferulic Acid Decarboxylases. *ChemcatChem* **2018**, *10*, 3736–3745. [[CrossRef](#)]
26. Annaval, T.; Han, L.; Rudolf, J.D.; Xie, G.B.; Yang, D.; Chang, C.Y.; Ma, M.; Crnovcic, I.; Miller, M.D.; Soman, J.; et al. Biochemical and Structural Characterization of TtnD, a Prenylated FMN-Dependent Decarboxylase from the Tautomycin Biosynthetic Pathway. *ACS Chem. Biol.* **2018**, *13*, 2728–2738. [[CrossRef](#)]
27. Payer, S.E.; Marshall, S.A.; Barland, N.; Sheng, X.; Reiter, T.; Dordic, A.; Steinkellner, G.; Wuensch, C.; Kaltwasser, S.; Fisher, K.; et al. Regioselective para-Carboxylation of Catechols with a Prenylated Flavin Dependent Decarboxylase. *Angew. Chem.-Int. Ed.* **2017**, *56*, 13893–13897. [[CrossRef](#)]
28. Marshall, S.A.; Payne, K.A.P.; Leys, D. The UbiX-UbiD system: The biosynthesis and use of prenylated flavin (prFMN). *Arch. Biochem. Biophys.* **2017**, *632*, 209–221. [[CrossRef](#)]
29. Payne, K.A.P.; Marshall, S.A.; Fisher, K.; Rigby, S.E.J.; Cliff, M.J.; Spiess, R.; Cannas, D.M.; Larrosa, I.; Hay, S.; Leys, D. Structure and Mechanism of *Pseudomonas aeruginosa* PA0254/HudA, a prFMN-Dependent Pyrrole-2-carboxylic Acid Decarboxylase Linked to Virulence. *ACS Catal.* **2021**, *11*, 2865–2878. [[CrossRef](#)]
30. Chen, R.B.; Gao, J.Q.; Yu, W.; Chen, X.H.; Zhai, X.X.; Chen, Y.; Zhang, L.; Zhou, Y.J.J. Engineering cofactor supply and recycling to drive phenolic acid biosynthesis in yeast. *Nat. Chem. Biol.* **2022**, *18*, 1032. [[CrossRef](#)]
31. Hou, Y.; Hossain, G.S.; Li, J.H.; Shin, H.D.; Du, G.C.; Chen, J.; Liu, L. Metabolic Engineering of Cofactor Flavin Adenine Dinucleotide (FAD) Synthesis and Regeneration in *Escherichia coli* for Production of alpha-Keto Acids. *Biotechnol. Bioeng.* **2017**, *114*, 1928–1936. [[CrossRef](#)] [[PubMed](#)]
32. Nagy, E.Z.A.; Nagy, C.L.; Filip, A.; Nagy, K.; Gal, E.; Totos, R.; Poppe, L.; Paizs, C.; Bencze, L.C. Exploring the substrate scope of ferulic acid decarboxylase (FDC1) from *Saccharomyces cerevisiae*. *Sci. Rep.* **2019**, *9*, 647. [[CrossRef](#)] [[PubMed](#)]
33. Khusnutdinova, A.N.; Xiao, J.; Wang, P.H.; Batyrova, K.A.; Flick, R.; Edwards, E.A.; Yakunin, A.F. Prenylated FMN: Biosynthesis, purification, and Fdc1 activation. *New Approaches Flavin Catal.* **2019**, *620*, 469–488.

Disclaimer/Publisher's Note: The statements, opinions and data contained in all publications are solely those of the individual author(s) and contributor(s) and not of MDPI and/or the editor(s). MDPI and/or the editor(s) disclaim responsibility for any injury to people or property resulting from any ideas, methods, instructions or products referred to in the content.